Int J Earth Sci (Geol Rundsch)
DOI 10.1007/s00531-014-1084-8

ORIGINAL PAPER

Coeval Lower Miocene subsidence of the Eisenstadt Basin and relative updoming of its Austroalpine frame: implications from high-resolution geophysics at the Oslip section (Northern Burgenland, Austria)

Hermann Häusler · Jürgen Scheibz · Werner Chwatal · Franz Kohlbeck

Received: 23 February 2014 / Accepted: 13 October 2014

Abstract A fault system southeast of Eisenstadt was investigated with high-resolution geophysics using electric resistivity tomography, seismics and gravimetry. The St. Margarethen Fault separates the Neogene succession of the Eisenstadt Basin from the north south-trending Rust Range, which belongs to the Austroalpine frame. The interpretation of profiles down to a depth of 350 m derived from reflection and refraction seismics combined with the density model along the Oslip road section clearly reveals a listric fault, which dips westward towards the Eisenstadt Basin. Bed thickness of growth-strata regularly increases from west to east, and normal fault drags visible in the seismic profile west of the St. Margarethen Fault allow for interpreting this structure as a hanging-wall syncline. Thickness distribution of Neogene deposits reveals that the Eisenstadt Basin can be interpreted as a half-graben bounded by the listric St. Margarethen normal fault, which developed at the western flank of Rust Range. The subsidence of the Eisenstadt Basin during Lower to Middle Sarmatian times was accompanied by concurrent updoming of the Rust Range of at least 70 m. For the mechanism of the updoming of the Rust Range footwall uplift during hanging wall subsidence is inferred.

Keywords Geophysics · Listric St. Margarethen Fault · Neogene Eisenstadt Basin · Rust Range · Coeval subsidence and updoming

H. Häusler (✉) · J. Scheibz
Department of Environmental Geosciences, University of Vienna, Vienna, Austria
e-mail: hermann.haeusler@univie.ac.at

W. Chwatal · F. Kohlbeck
Department of Geodesy and Geoinformation, Vienna University of Technology, Vienna, Austria

Introduction

The Neogene Eisenstadt Basin, the Austrian sub-basin of the Eisenstadt-Sopron Basin, is located southeast of the Vienna Basin. It is 20 by 20 km in size and bordered by the Leitha Mountains to the north, the Rosalia Mountains to the west, the Sopron Mountains to the south, and the Rust Range to the east. The Rust Range continues south to Fertőrakos in Hungary. From a geomorphic point of view the Eisenstadt Basin is termed Wulka Basin since the River Wulka discharges to Lake Neusiedl in the east (Fig. 1).

Geophysics and deep drilling were widely used for hydrocarbon exploration and prospection in the Vienna Basin. Compared to the Vienna Basin, which can be termed a mature basin (Häusler et al. 2002; Wessely 2006), the relatively shallow Eisenstadt Basin did not yield hydrocarbons (Feichtinger and Spörker 1996), and therefore data from more intensive geophysical- and drilling-campaigns is missing.

Aside from a few deep seismic sections acquired by Austrian hydrocarbon companies such as Rohöl-AG (RAG) in the 1950s and Österreichische Mineralölverwaltung (OMV) in the 1970s, geophysical investigations for analyzing the faults along the Austroalpine basement bordering the Eisenstadt Basin were hardly applied. Based on these few seismic cross sections and one exploration well drilled in 1945 to a depth of 1,415 m (Zillingtal 1), Kröll and Wessely (1993) extended the structural map of base Neogene from the Southern Vienna Basin to the Eisenstadt-Sopron Basin. Referring to the general geometry of the basin fill, which varies from 400 to 600 m in depth in front of the Rust Range to 2,000 m in its western part in front of the Rosalia Mountains, the basin shows an asymmetric geometry, gradually deepening to the southwest (Salcher 2008; Salcher et al. 2012). Figure 2, which

Published online: 02 November 2014

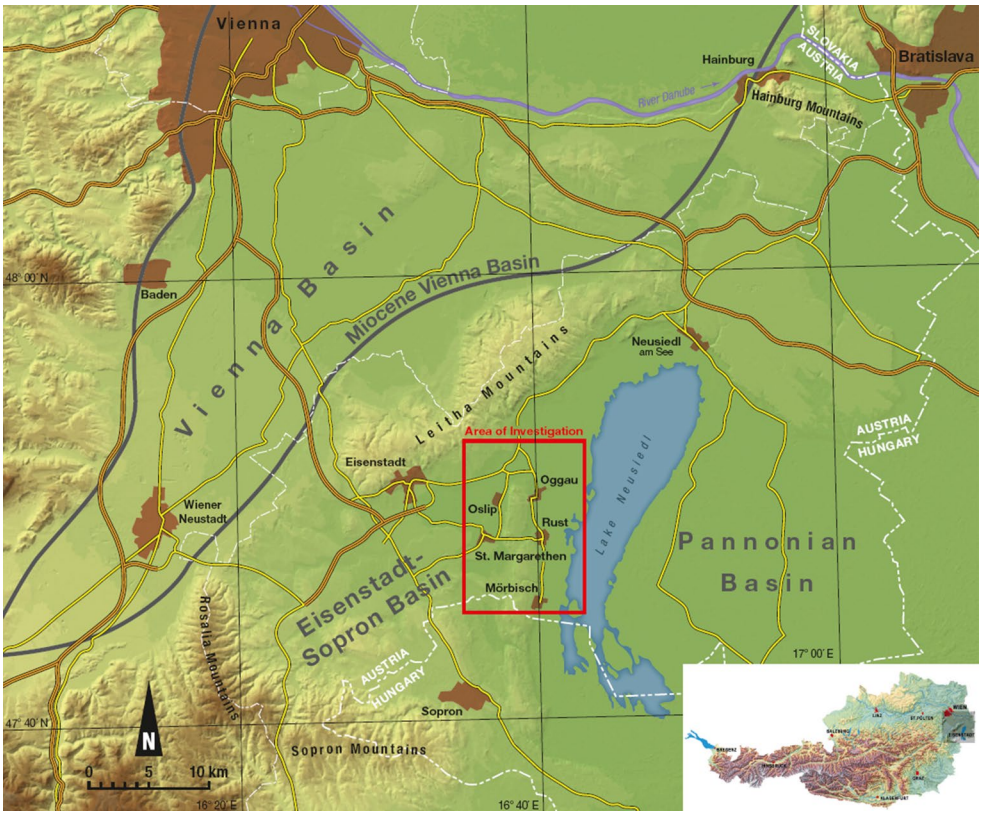

Fig. 1 Map of Eisenstadt-Sopron Basin with area of investigation west of Lake Neusiedl approximately 60 km southeast of Vienna

depicts geological sections from the southern Vienna Basin to the Eisenstadt Basin and from the Eisenstadt Basin to the Pannonian Basin, was drawn based on geological maps 1:50,000 (Herrmann et al. 1993; Brix and Pascher 1994) and a structural map base of Neogene 1:200,000 (Kröll and Wessely 1993).

Decker (1996), Decker and Peresson (1996), Peresson and Decker (1996, 1997) and Decker et al. (2005) published very detailed structural analyses in the Alpine-Carpathian-Pannonian transition zone. Tectonic structures of the Eisenstadt Basin were reported by Sauer et al. (1992a, b), and recently reinvestigated e.g. by Exner et al. (2008), Exner and Grasemann (2010), Rath et al. (2011), Spahić et al. (2011), and Exner and Rath (2012). The rollover and hanging-wall collapse structure, which was reported from the gravel pit of St. Margarethen–Gemeindewald by Decker and Peresson (1996), was reinterpreted by Spahić et al. (2011), who favored a planar geometry instead of a listric fault geometry of the structures studied at the same gravel pit, partly because no weak layer serving as a ductile detachment horizon could be identified there. A special study on fault tectonics, in particular on neotectonics of the Mönchhof Fault east of Lake Neusiedl, was performed by Székely et al. (2009). Information on the evolution of the Eisenstadt-Sopron Basin is scarce, but the Eisenstadt Basin cannot be termed a pull-apart basin when compared to the structural evolution of the Vienna Basin (Strauss et al. 2006; Hölzel et al. 2008, 2010) because of the missing prominent strike-slip faults.

During investigations for compiling the explanations of geological maps 1:50,000, previously published by the Geological Survey of Austria, many outcrops of Northern Burgenland were re-studied by Häusler (2007, 2010, 2012a, b), and several fault zones were newly investigated (Scheibz 2006, 2010; Scheibz et al. 2008a, b, 2009; Kardeis 2009; Häusler et al. 2007). In addition, aerogeophysical (Ahl et al. 2012) and near subsurface geophysical investigations were conducted and proved to be very useful for hydrogeological campaigns and water supply (e.g. Kollmann 2005; Häusler et al. 2008a, b; Scheibz et al. 2008a, b). This information provides valuable local insights to the facies of Neogene deposits, which can change rapidly in both lateral and vertical directions.

In order to study shallow and deep structures along the Rust Range bordering the Eisenstadt Basin to the east, complementary high-resolution geophysical methods along the same profile perpendicular to the north–south-striking fault zone were applied. Shallow geophysical profiles down to approximately 30 m (gained by electric resistivity tomography) together with results from seismics and gravimetry down to several hundred meters, local geologic mapping of Neogene formations and profiles from local drilling were all used for geologic interpretation and linking. Evidently, the best results for interpretation of ERT

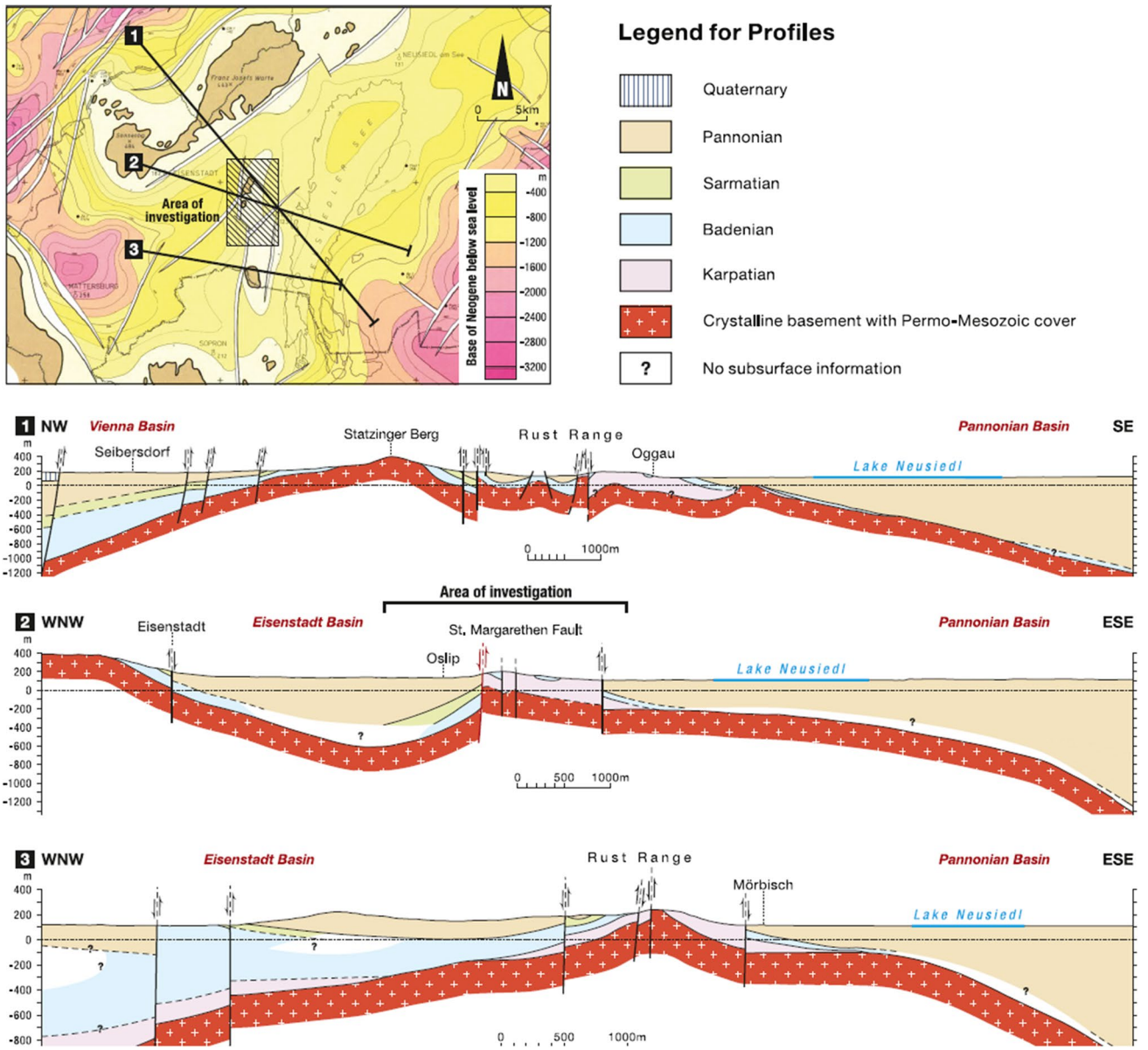

Fig. 2 Geological sections across the Rust Range (modified from Häusler 2010) with an insert of structural map base of Neogene modified from Kröll and Wessely (1993) depicting outcrops in the surroundings of Eisenstadt Basin in *brown*

profiles can be gained where benchmark profiles comparing ERT with geological profiles in adjacent outcrops are available (Smith and Sjogren 2006).

Regional geologic setting

In this paragraph stratigraphy, lithology and facies relevant to the interpretation of geophysical profiles are briefly described, especially the Austroalpine crystalline basement of the Rust Range and its Neogene to Quaternary cover (Fig. 3). The geological map 1:50,000 was compiled by Herrmann et al. (1993), and the explanations were published by Häusler (2010). For biostratigraphic results Fuchs (1960) is referred to and more details about the local geology of the Rust Range and its vicinity can be found in Fuchs (1965).

Crystalline basement

Despite ongoing discussions on the tectonic position of the Rust Range (Schuster 2010), the crystalline complex of the Leitha Mountains and Rust Range belongs to the Austroalpine basement in the sense of Tollmann (1977). The crystalline of the Rust Range consists of metamorphic

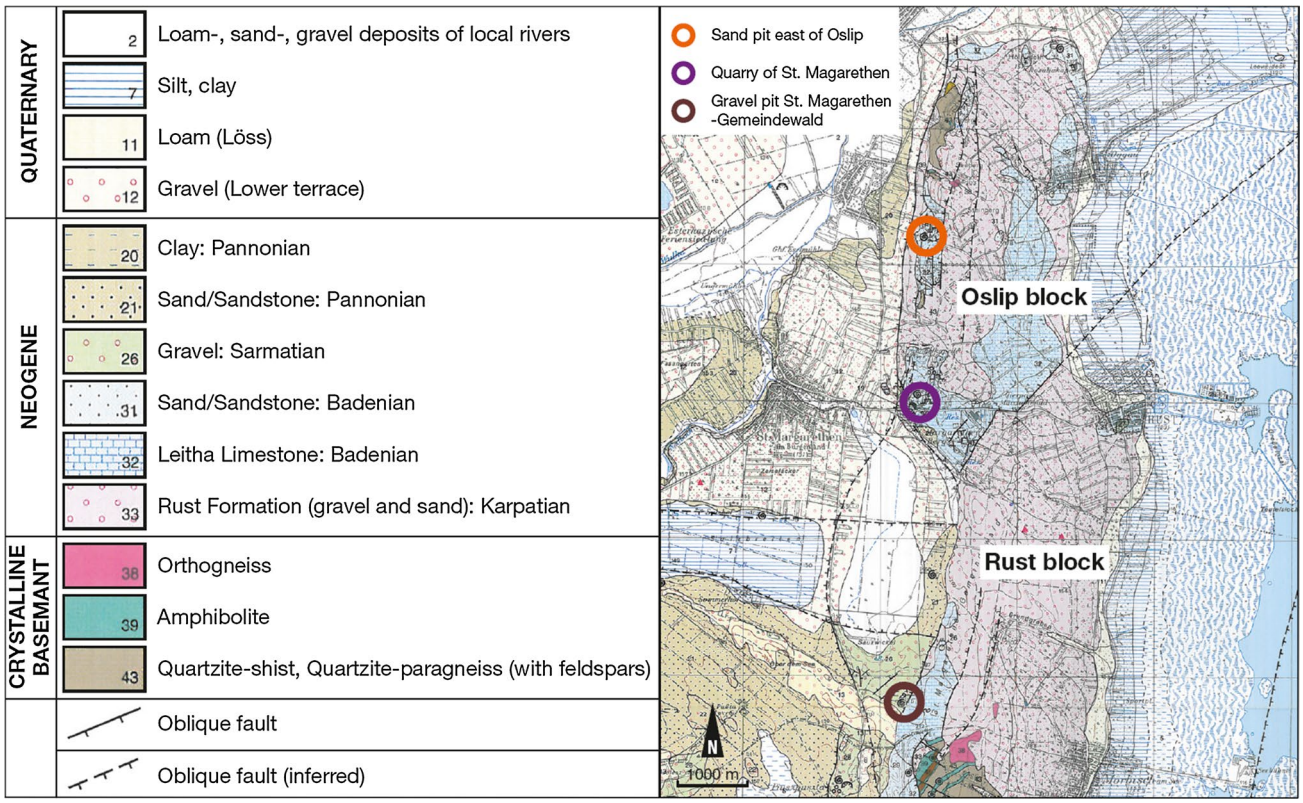

Fig. 3 Detail of geologic map 1:50,000 with deposits of Neogene to Quaternary age covering the Austroalpine crystalline basement of the Rust Range modified from Herrmann et al. (1993). The north–south trending fault northeast of St. Margarethen is termed the St. Margarethen Fault. *Circles* highlight sand pits and quarries featuring sedimentary and tectonic structures

Paleozoic rocks. The basement crops out in two smaller areas only, namely in the north of the Rust Range, northeast of Oslip and in the south, close to the Hungarian border. A series consisting of quartzite shists, paragneiss including amphibolite layers and biotite gneiss as well as intrusions of granitic orthogneiss was mapped west of Mörbisch. The quartzite shists in the quarry west of Mörbisch are folded, faulted and deeply weathered (Fig. 4). Except for these smaller areas of crystalline rock formations, the entire Rust Range is covered by Neogene deposits mainly comprising the Rust Formation of Karpatian age.

Neogene formations

The remnant of the former Tethys Ocean north of the European alpine belt is termed Paratethys. Its central basin (termed Central Paratethys) flooded both the Vienna Basin and its southeastern satellite basin, the Eisenstadt-Sopron Basin. Their Neogene stratigraphy is based on paleobioprovinces—due to remarkable facies dependences of faunas and migrations of endemic mollusc faunas (Sacchi and Horváth 2002)—the use of chronostratigraphy is not valid for the whole Central Paratethys. Dating of marine, deltaic and fluvial deposits in the Eisenstadt Basin is based on biozones, which are summarized in Table 1. The differing local paleogeographic conditions from Karpatian to Pannonian times, sedimentation in shallow marine, deeper marine, fluvial to lacustrine environments, rapid facies change at short distances and synsedimentary faulting all complicate the interpretation of geophysical profiles. In addition, sea-level fluctuations have caused intra-Badenian unconformities as well as major unconformities at the base of Sarmatian- and Pannonian-formations. Except for the Rust Formation no formal nomenclature system has been established for younger formations in that region so far. Miocene formations of the Central Paratethys were studied in the Rust Range comprising formations of Badenian to Sarmatian age and formations of Pannonian age. Table 1 gives a schematic overview on age, lithology and facies of Lower to Upper Miocene strata referred to in text and interpretation. The very detailed paleontological studies of Fuchs (1960) allow for a precise comparison of marine formations based on (benthic) foraminifera, or e.g. shallow water deposits, based on mollusc biozones.

In the Rust Range the terrestrial, mainly fluvial Rust Formation (Fuchs 1965) overlies the crystalline basement. Due to missing biostratigraphic evidence it is not clear, however, if the siliciclastic Rust Formation, which is

Fig. 4 Outcrop of quartzite shists of the Austroalpine basement in a quarry on top of the southern Rust Range, west of Mörbisch. The Paleozoic formation is locally strongly deformed along faults, and deeply weathered

traditionally dated as of Karpatian age (Fuchs 1965; Tollmann 1985; Häusler 2010), partly could be equivalent of the fluvial Aderklaa Conglomerate of Lower Badenian age (Strauss et al. 2006).

Lithology of the Rust Formation differs widely, consisting of matrix supported sandy gravel or gravelly sand, with size of the weathered crystalline components varying between cm-, dm- and up-to several meters in diameter. Its maximum thickness is estimated to be 100 m although drilling and seismic exploration of this formation in the Rust Range is missing. Nowadays the Rust Formation can only be observed at construction sites. Grain size analysis of several samples taken at a construction site west of Mörbisch characterizes the Rust Formation as sandy gravel (Fig. 5). For the interpretation of ERT sections it is worth knowing that the Rust Formation acts as an aquifer for highly mineralized groundwater, rich in potassium (Sauerzopf 1962; Schmid 1968).

Marine ingression of the Eisenstadt Basin commenced in Middle Badenian times (Upper Lagenida zone, Table 1). In the central and eastern part of the Rust Range the Rust Formation is overlain by Leitha Limestone, a massive to thick-bedded carbonate rock varying from 40 to 110 m in thickness (Fuchs 1965). In Badenian times, the coralinacean Leitha Limestone facies was a shallow-water marginal facies deposited along the islands and atolls of the Leitha Mountains and the Rust Range. Leitha Limestone on top of the Rust Range is of Middle Badenian age. Its base is located at an altitude of 200 m above sea level and limestone beds equivalent in age crop out at the eastern and western sides of the Range at an altitude of 130 m. Consequently, an uplift of the Rust Range of about 70 m took place post-Middle Badenian age. Leitha Limestone of Lower Sarmatian age (*Elphidium reginum*-Zone; Table 1) is locally preserved at the western margin of the Rust Range near St. Margarethen (Küpper 1957) and at its eastern margin near Rust. Due to the fact that transgressive fossiliferous sand- and gravel-beds of Upper Sarmatian age unconformably overly cliffs of Leitha Limestone of Badenian age near St. Margarethen and north of Oggau, Fuchs (1965) deduced an uplift of the Rust Range in two steps: the first in Upper Badenian times, and the second during Middle Sarmatian times, which is when the present day geomorphology of the Rust Range was fundamentally shaped.

Since limestone was mined in many quarries east and north of St. Margarethen, Fuchs (1965) termed the northern part of the Rust Range "Quarry block" ("Steinbruchscholle"), and the southern block, mainly comprising Rust Formation, "Rust block" ("Ruster Scholle"). For regional descriptions the term "Rust block" is used further on, but instead of quarry block near Oslip the term "Oslip block" is preferred (Fig. 3). When both the Oslip and Rust blocks were uplifted along north–south trending faults, slices of the Rust Range comprising Neogene deposits were tilted to the east and southeast. Compared to the section of Fig. 51 in Sauer et al. (1992b) this tilting to the east matches the young subsidence of the Pannonian Basin.

Due to intensive mining of limestone and gravel during the last century, synsedimentary structures as well as local horizontal and vertical facies change were well documented from outcrops or can still be studied in sand pits and quarries (Häusler 2010; Wiedl et al. 2012). This is also true for the quarry east of St.

Margarethen (Fig. 6), the sand pit east of Oslip (Fig. 7) or the gravel pit of the St. Margarethen–Gemeindewald SSE of St. Margarethen (Fig. 8). Drillings in the Neusiedl Basin east of the Rust Range revealed that Neogene deposits of e.g. Badenian and Sarmatian age are missing there because subsidence of the Danube Basin (as part of the western Pannonian Basin) did not commence prior to Pannonian times (Harzhauser and Piller 2005). Abundant steep north–south-tending faults in quarries of St. Margarethen reveal dip slip of hanging wall blocks towards the Eisenstadt Basin (Fig. 6b, c), which represent very young to recent tectonic activity (Kieslinger 1955, 1960) (Fig. 9).

The transition of proximal limestone facies to more distal coarse-clastic facies was studied in the Oslip quarry, southeast of Oslip. The Leitha Limestone of the old

Table 1 Bio- and litho-stratigraphy of Miocene deposits in the surroundings of the Rust Range according to Fuchs (1960, 1965)

Time of Tops (My)	Epoche	Classical Stages	Central Paratethys Stages *This Study*		Biozones: Benthic foraminifera	Biozones: Molluscs		Lithology	Facies
7,8	Upper Miocene	Tortonian	Pannonian	Upper	Absent due to brackish and limnic environment)	H G F	*Viviparus; Congeria rhomboidea* *Mytilopsis neumayri* (∞ *Congeria neumayri*) *Mytilopsis zahalkai* (∞ *Congeria zahalkai*) *Congeria praerhomboidea*	Coarse clastic deposits, clay; lignite	Limnic Brackish
10,0				Middle		E D	*Congeria subglobosa* *Congeria partschi*	Sand, marl, clay	
10,5				Lower		C B (A)	*Mytilopsis hoernesi* (∞ *Congeria hoernesi*) *Mytilopsis ornithopsis* (∞ *Congeria ornithopsis*) *Melanopsis impressa*	Gravel, sand, marl, clay	
11,6	Lower Miocene	Serravallian	Sarmatian	Upper	*Porogranonion granosum* (∞ *Nonion granosum*)		*Mactra*	Gravel, sand	Marine
				Middle	*Elphidium hauerinum*		*Ervilia*	Detrital Leitha Limestone, gravel, sand (marl)	
12,2				Lower	*Elphidium reginum*, *Anomalinoides dividens*		*Mohrensternia* (∞ *Cerithia*)	Detrital Leitha Limestone	
12,7		Langhian	Badenian	Upper	*Rotalia Bulimona-Bolivina*		Abundant without zonation	Deposits missing due to regression	Marine
13,6				Middle	*"Sandschaler Zone", Spiroplectammina*			Leitha Limestone, gravel, sand, marl	
16,1				Lower	*Lagenida*			Marine ingression; Rust Formation resedimented	
16,3		Burdigalian	Karpatian		No fossil record			Rust Formation (gravel, sand)	Terrestric

Biozonation of Badenian and Sarmatian is based on molluscs (zone A–H) of the shore- and delta-deposits, and on benthic foraminifera of deeper water deposits. Central Paratethys stages and facies for comparison are compiled from Harzhauser et al. (2002), Harzhauser and Tempfer (2004), Harzhauser et al. (2004), Piller and Harzhauser (2005). Former nomenclature of species (∞ equivalent) is in parenthesis and time axis is to scale. Tops of stages of the Central Paratethys are taken from Hölzel et al. (2010). Red star indicates tectonic uplift of Rust Range between Upper Badenian and Upper Sarmatian times

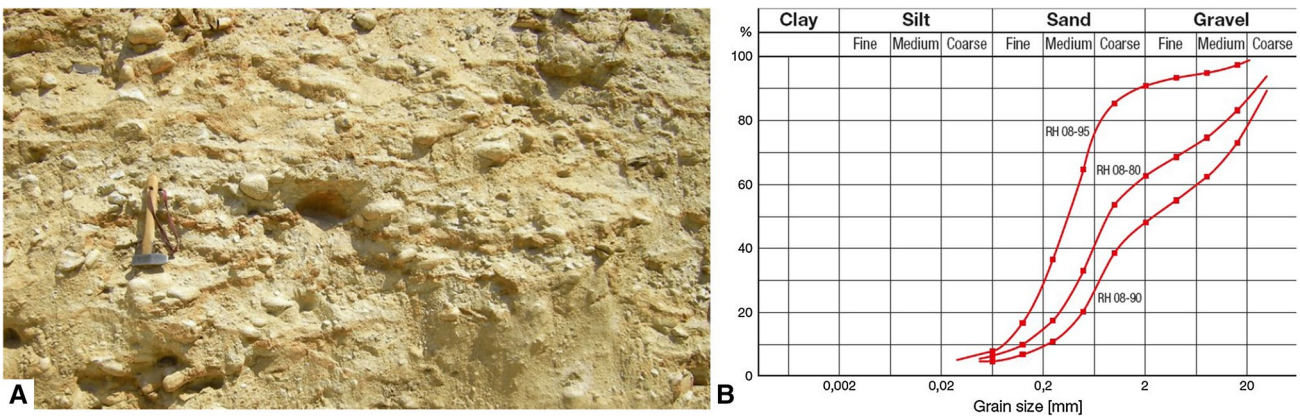

Fig. 5 Outcrop of sand-supported gravel of Rust Formation of Karpatian age (**a**) from a construction site west of Mörbisch, and grain size analyses of three samples (**b**), modified from Häusler (2010)

Silberberg quarry (Fig. 10) continues north of the road Oslip–Rust, and therefore the southern part of the Oslip outcrop (Fig. 7) is a quarry in massive limestone facies. The limestone beds disintegrate to the north, and then comprise of meter thick sedimentary breccia beds, which change to cm-thin-bedded layers of coarse sand, rich in clasts of the eroded basement of the Rust Range (Fig. 7c, d).

In the Oslip sand pit, thick-bedded limestone facies (Fig. 7a) is underlain by fine sand of 15–20 m in thickness (Fuchs 1965), which belongs to the "Sandschaler Zone" (Table 1). Since the sand facies prevails in this outcrop it is termed sand pit (SG = "Sandgrube") in the topographic map. The sand is rich in deformation bands, which reveal decimeter-scaled graben- and horst-structures (Fig. 7b).

Fig. 6 Massive, bright Leitha Limestone of Badenian age is preserved in the St. Margarethen quarry (**a**) with steep faults paralleling the St. Margarethen Fault. Within the central quarry, in the area named "Ringstrassen Areal", bending of limestone beds along steeply west dipping normal faults (**b**) and striations (**c**) on steep slicken sides indicate dip slip of hanging wall to the west, down to the Eisenstadt Basin. Today this old part of the quarry serves for opera festivals

The Oslip sand pit (partly quarry) gives an excellent insight to rapid vertical and lateral change of sedimentary facies, the knowledge of which is useful for interpretation of shallow geophysical profiles, in particular resistivity tomography. For this reason a special study was performed by Kardeis (2009), who measured an ERT profile east of the Oslip sand pit (Fig. 11).

In the entire central Eisenstadt Basin the Badenian limestone facies is replaced by a coarse clastic sandy to gravelly facies. The facies development during Badenian times passed to Sarmatian times. The limestone formation of Badenian age, rich in corals and algal colonies, was eroded and redeposited and therefore succeeded by dendritic Leitha Limestone, and the coarse clastic delta facies was deposited in the neighbouring Eisenstadt Basin. The gravel of the gravel-pit of the St. Margarethen–Gemeindewald is rich in fossils of Upper Sarmatian age (*Nonion granosum*-Zone), and locally cemented to conglomerates (Fig. 8a). In the 25 m high southern wall the thickness of the growth-strata regularly increases from west to east, and also the dip of the bedding planes increases in the same direction (Decker and Peresson 1996, Fig. 3).

Marine gravel deposits of the gravel pit of the St. Margarethen–Gemeindewald represent thick beds of this transgression of the *Nonion granosum*-zone of Upper Sarmatian age. At both the St. Margarethen quarry and the St.

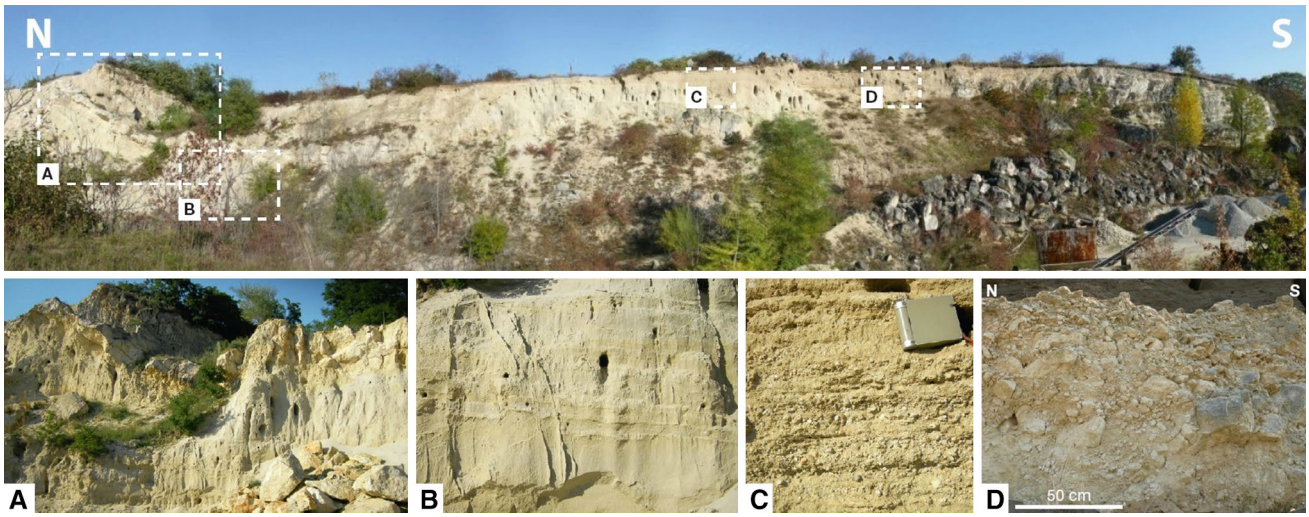

Fig. 7 In the sand pit east of Oslip massive Badenian Leitha Limestone vertically and laterally changes into a coarse clastic facies. In the north the locally 30° eastwards dipping limestone beds (*A*) are underlain by sand associated with typical deformation bands (*B*). The massive limestone laterally changes into coarse debris facies (*D*) and further north into thin-bedded coarse sand (*C*). Panorama of 200 m long northeastern wall of Oslip sand pit courtesy of Gerhard Kardeis; photographs of outcrop details taken by Hermann Häusler

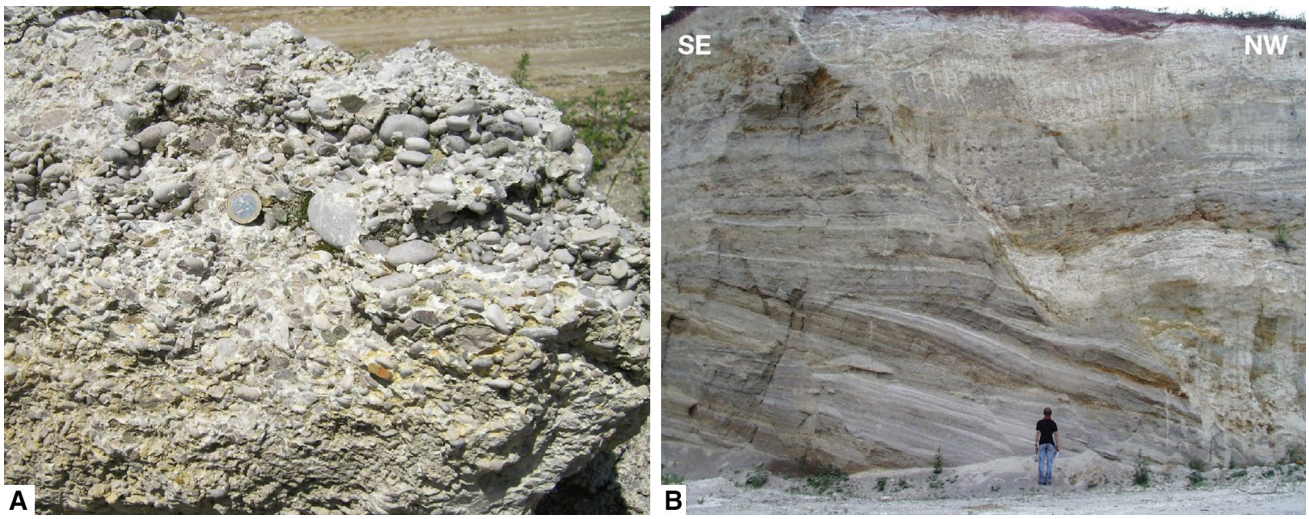

Fig. 8 Coarse-clastic deposits rich in fossils of Sarmatian age in gravel pit St. Margarethen–Gemeindewald. Gravel beds locally are cemented and form conglomerates (**a**). In 2008 the outcrop conditions allowed the mapping of a prominent, no planar, curved and steeply northwestward dipping fault (**b**), which corresponds to the NW-dipping fault close to the sand pit in the geological map

Margarethen gravel pit locations, fine clastic beds of Lower Pannonian age (molluscs-zone B) conformably overly the sand and gravel deposits of Upper Sarmatian age at the western side of the Rust Range (Fuchs 1965). Basically, sedimentation and subsidence in the Eisenstadt Basin commenced until Middle Pannonian (molluscs zone D, E), limnic deposits rich in lignite beds are predominantly known from the transition zone between Eisenstadt Basin and Southern Vienna Basin (Neufeld Formation), and from the Neusiedl Basin east of the Rust Range (Fuchs 1965).

Before enlargement of the gravel pit located in the St. Margarethen–Gemeindewald, Decker and Peresson (1996) as well as Spahić et al. (2011) studied abundant sedimentary structures. The geometry of the main fault separating the Sarmatian beds from the Badenian Leitha Limestone and the Rust Formation (Fig. 3) was interpreted conversely, however. Decker and Peresson (1996) interpreted this fault as a listric fault, whereas Grasemann et al. (2004, 2005) and Spahić et al. (2011) interpreted it as a planar fault. Within the scale of that gravel pit, Decker and Peresson

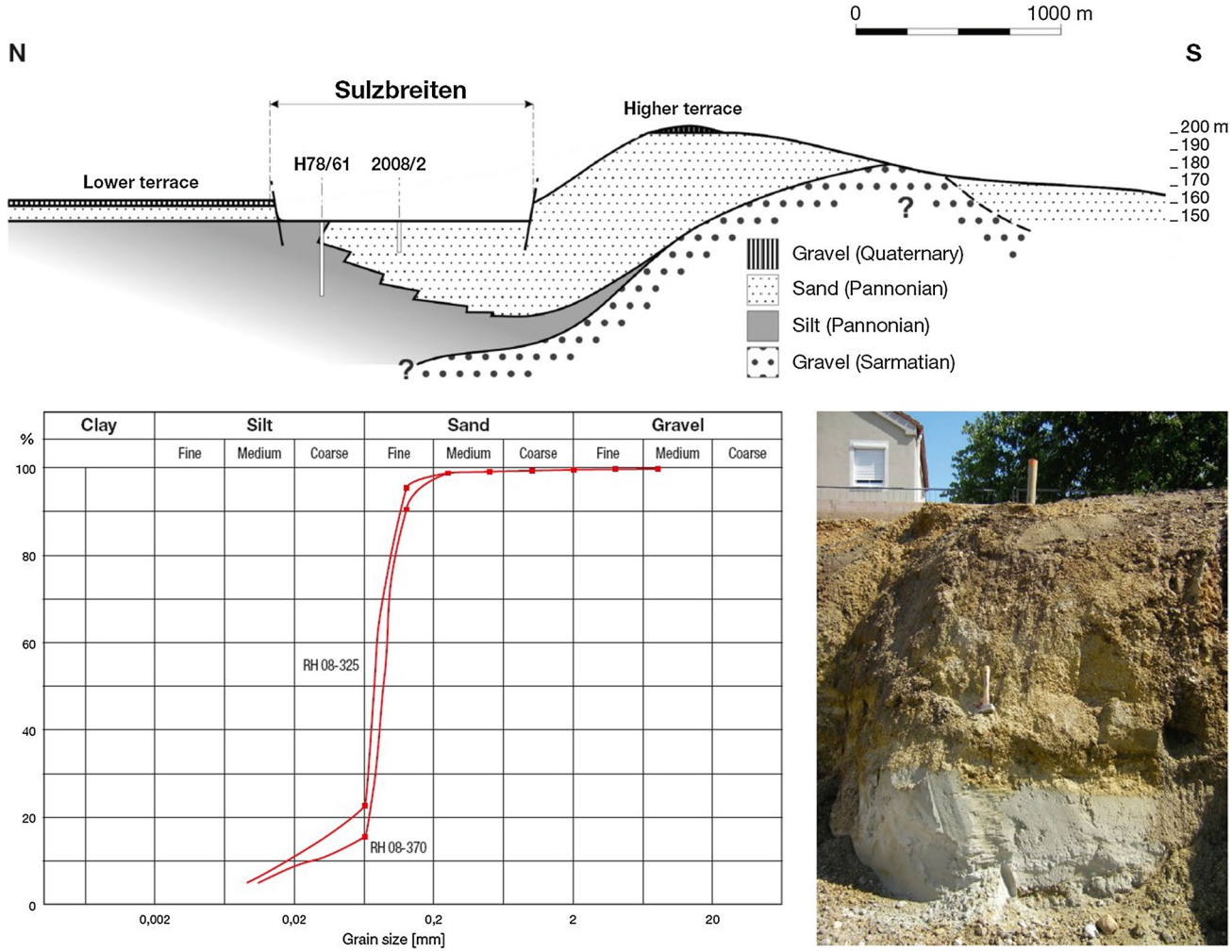

Fig. 9 Rapid *horizontal* and *vertical* facies change from sandy to clayey facies of Pannonian age in the Sulzbreiten, the depression south of St. Margarethen (modified from Häusler 2010). Insert depicts grain size analysis of two samples from borehole drilling campaign in 2008. Southeast of St. Margarethen, brownish gravel of Pleistocene age overlies this white fine sand of Pannonian age

(1996) documented a fan-shape pattern typical for growth-strata with bed thicknesses regularly increasing from west to east, and strata dipping towards a master fault with dip angles steepening from west to east. They interpreted the hanging-wall collapse, exposed in a section of the St. Margarethen–Gemeindewald gravel pit of approximately 25 m in thickness, as a rollover structure along a WNW-dipping listric fault. More recently, Pretsch (2009) and Spahić et al. (2011) reinterpreted this synsedimentary fault structure of the gravel pit in the St. Margarethen–Gemeindewald, favoring a local fault drag along a planar fault instead of a rollover anticline related to a listric fault. At a former outcrop of the northwestern wall of the gravel pit of the St. Margarethen–Gemeindewald, a curved fault dipping in northwestern direction was visible (Fig. 8b).

Spahić et al. (2011, Fig. 7c) also applied the displacement gradient model at the Oslip sand pit, and interpreted the fault in front of limestone beds, which locally are dipping 30° to the east, as reverse drag along a planar fault associated with the deformation bands in the footwall of the normal fault.

Since there are no more brick factories active in the region, outcrops of Pannonian clay deposits in the center of the Eisenstadt Basin are rare, and borehole drilling and shallow geophysical sounding for hydrogeological investigations mainly document the distribution of the Pannonian clay facies. In the Sulzbreiten, a geomorphologic depression south of St. Margarethen, the deposits of Middle Pannonian times (Zone D, E; Fuchs 1965) are represented by white fine sand, which was drilled down to 20 m in 2008 (Häusler 2010). In the eastern Eisenstadt Basin, sand and marl of Middle Pannonian age are overlain by fluvial deposits of Quaternary age rich in brownish quartzite pebbles of few cm in diameter (Higher and lower terrace, Fig. 9).

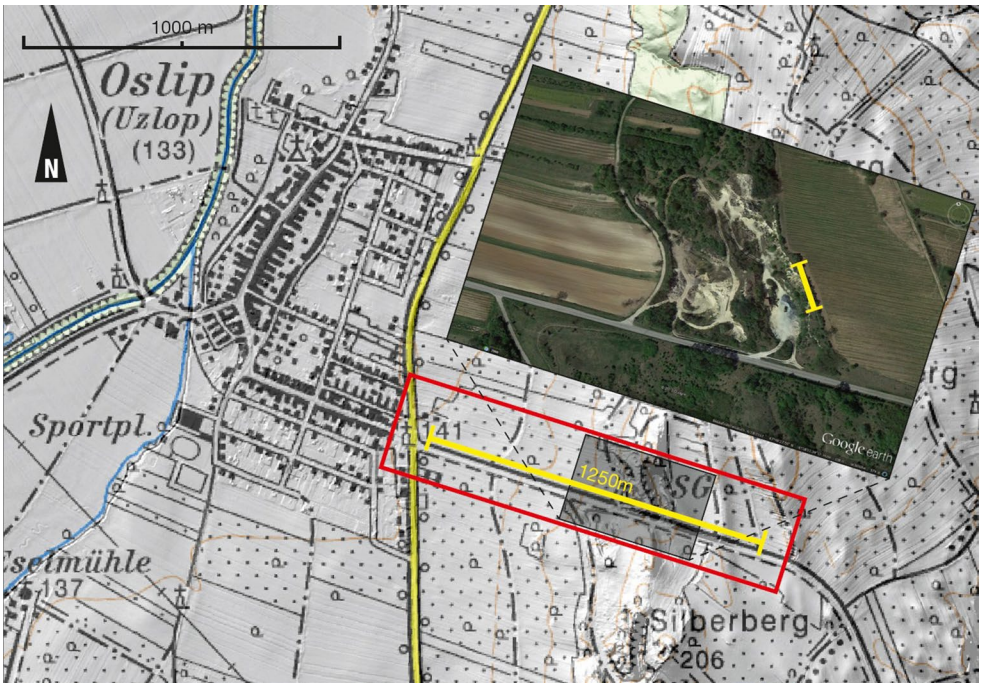

Fig. 10 Location of geophysical survey along the road Oslip–Rust with beginning opposite shrine at survey point 141 (*yellow line* in *red rectangle*). Topographic map at original scale 1:50,000 (courtesy: BEV) with insert of satellite image of the sand pit (*SG* "Sandgrube") Oslip, and orientation of 100 m long ERT profile measured on top of the wall of the sand pit (*yellow line* in Google Earth)

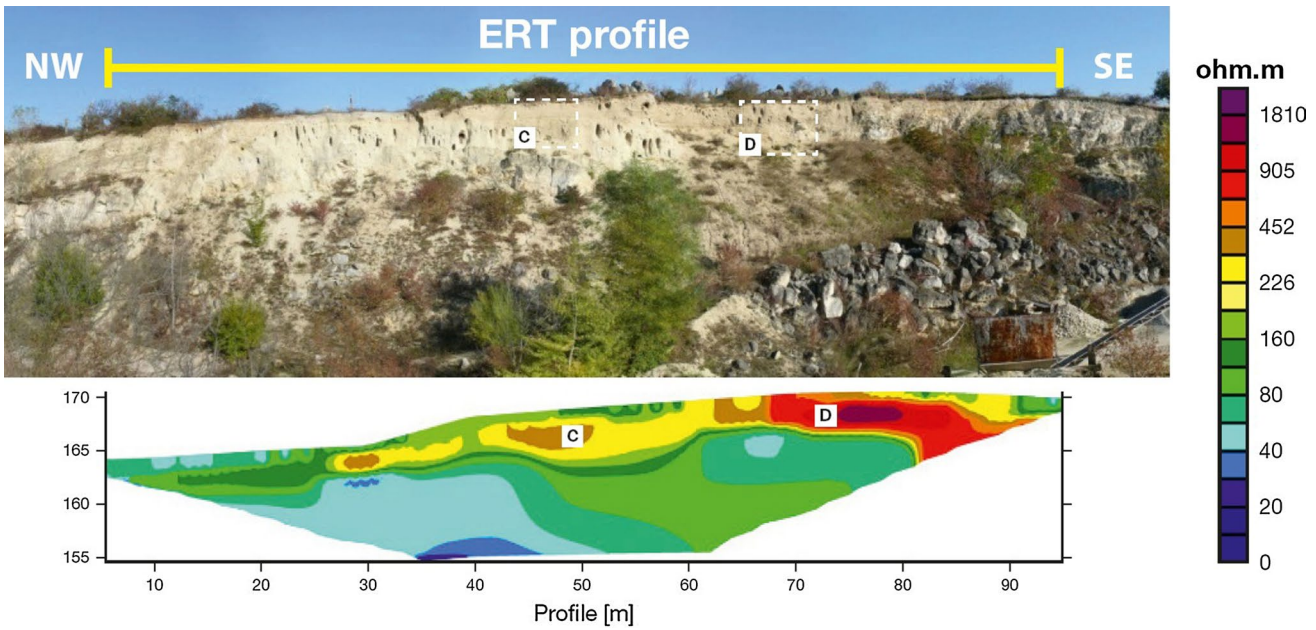

Fig. 11 The 100 m long ERT profile was taken on top of the eastern wall of the Oslip sand pit. For location see Fig. 10. The inversion profile is modified from Kardeis (2009). It reveals higher resistivities of Leitha Limestone and its coarse clastic debris (*D*) and lower resistivity of thin-bedded layers of sand and gravel (*C*), which emplace the limestone facies to the northwest

Geophysical methods

The combination of complementary geophysical methods enables a profound interpretation tool since different physical properties of the subsurface can be correlated. To obtain a full high resolution image from a few meters down to a maximum of 350 m depth the following methods were applied: electrical resistivity tomography (ERT), seismics and gravimetry (Table 2).

For direct comparison of the results, all these methods were applied along one profile southeast of Oslip, perpendicular to the north–south trending St. Margarethen Fault (Fig. 9). In addition, a 100 m long ERT profile with 2 m electrode spacing paralleling the wall of the Oslip sand pit

Table 2 Parameters of field measurements for the different geophysical methods, length and sensor spacing along the road Oslip–Rust, southeast of Oslip Village

Methods	Profile length (m)	Sensor spacing (m)	Device
ERT	1,250	4.0	GEOTOM4MK100
Seismics	770	4.0	DMT Summit II
Gravimetry	1,250	10.0	Scintrex-CG3

was measured, where resistivities could directly be interpreted compared to lithology of the pit (Fig. 11). All geophysical profiles were geodetically surveyed.

Electrical resistivity tomography (ERT)

ERT measurements were carried out using the GEOTOM4MK100 equipment manufactured by GEOLOG2000 with 100 electrode takeouts. The greatest depths to which resistivities can be interpreted depend on the farthest distances between current and potential electrodes of single measurements. For this study the Wenner- and Schlumberger-configuration was used since horizontal facies changes of Neogene formations in the Oslip sand pit were mapped. Measurements were conducted with 1 m electrode spacing leading to a layout of 100 m of the shorter profile above the Oslip sand pit (Fig. 11) and with 4 m electrode spacing leading to a layout of 400 m of the longer profile. For the latter the roll along technique with 50 % overlap was applied (Fig. 12).

The data was quality controlled in the field and thereafter filtered and inverted with the RES2DINV software (Loke 2004) using the Gauss–Newton method (DeGroot-Hedlin and Constable 1990). For the inversion process the software calculates a model solving smoothness constrained least-squares method. A root mean square error (RMS) is calculated from the difference between the apparent resistivities obtained from the measurements and the apparent resistivities calculated from the model. Geodetic survey of ERT data points enabled the incorporation of the topography into the model using the option of the inverse Schwartz–Christoffel method (Loke 2004; Spiegel et al. 1980). This achieves the most accurate layer thickness for flat gradients. In this study all inversions were converged to an RMS-error of 3–6 % within five iterations. The final results were displayed using Surfer software.

Refraction- and reflection-seismics

Data-acquisition along the Oslip section was done with 144 channels of the Summit II system from DMT Company with a geophone spacing of 4 m. As a seismic source a pneumatic hammer (Vakimpak) was used with a shot interval of 8 m leading to average common depth point (CDP)-fold of 35 traces. The seismic data was processed with ProMAX® (Landmark Graphics Corp.) including standard processing, as automatic gain control (AGC), spiking deconvolution, bandpass filter, velocity analysis, normal move out (NMO)-correction, CDP-stacking, and depth migration for the reflection seismics. To get a better image of the nearly vertical faults dip move out (DMO)-correction instead of the NMO-correction was applied. The refraction tomography was calculated with Software Rayfract™ (Intelligent Resources Inc.), which uses the wavepath eikonal traveltime tomography (WET, Schuster and Quintus-Bosz 1993) to calculate the seismic velocities. The final result is a seismic depth section consisting of a reflection seismic image to a maximum depth of 350 m and the velocity distribution of the refraction tomography down to a maximum depth of 80 m below surface.

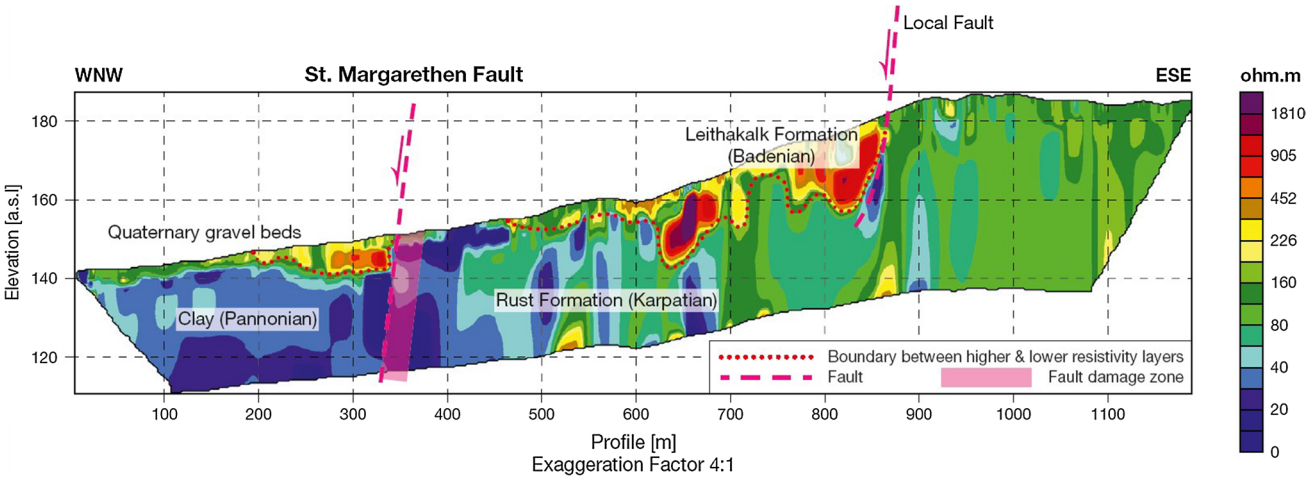

Fig. 12 1,250 m ERT profile of Neogene deposits of the road section Oslip–Rust, along with structural interpretation. For location see Fig. 10

Table 3 General resistivities in ohm m of non water-saturated soft- and hard-rocks

Resistivity (ohm m)	Lithology
<50	Marl, clay
50–100	Sandy marl and clay
100–200	Clayey sand
200–400	Sand
400–1,000	Gravel
>1,000	Hard rock, e.g. limestone

Gravimetry

Finally, a gravimetry survey using a Scintrex-CG3 gravimeter (capable of automatically eliminating the earth tide correction) with a spacing of 10 m was performed. To get the drift of the gravimeter, the survey was carried out as a loop, which means that the measurement began and ended at a base station. By means of detailed surveying, the free air and latitude corrections were calculated and the topographic correction was determined from a Digital Terrain Model with a raster of 25 m. After applying the aforementioned corrections a Bouguer-anomaly was obtained from which a density model of the underground could be derived.

Results

For the geologic interpretation of near surface geophysics such as ERT, the local knowledge of facies development and facies changes of the Neogene deposits as well as its groundwater distribution is essential. To sum up, the lithology of the Rust Formation of Karpatian age overlying the crystalline basement can rapidly change from sandy gravel to gravelly sand, and the size of the weathered components can also vary significantly locally. Therefore, resistivity of faulted and weathered crystalline of the Rust Range may resemble the resistivity of the Rust Formation. The facies of Badenian deposits of the area Oslip–St. Margarethen also changes rapidly either vertically or horizontally when the limestone facies changes to coarse clastic and fine clastic facies. The Leitha Limestone of Badenian to Sarmatian age is karstified but natural springs hardly occur in the Rust Range. The timely equivalent sand and gravel facies of the Eisenstadt Basin, however, is an important aquifer for drinking water supply. In general, the Pannonian deposits are clayey and therefore act as confining beds except for the area south of St. Margarethen, where a porous aquifer consisting of fine sand prevails. ERT profiles therefore reflect lithology, permeability, and groundwater mineralization of the Neogene formations.

ERT

In conclusion of knowledge on rapid lateral and vertical change of the Neogene facies, as described above, the ERT profile of the Oslip sand pit is presented as a benchmark for interpreting the ERT profile crossing the St. Margarethen Fault (Fig. 12). Table 3 gives an overview of the resistivity parameters of the formations in the investigated area.

ERT profile east of the Oslip sand pit

The 100 m long high resolution ERT profile was conducted 15 m east of the eastern wall of the Oslip sand pit, paralleling the 15 m high outcrop in a northwestern direction (Fig. 11). This enabled direct correlation of resistivity patterns of the ERT profile both with the lithology of the sand pit and with the lateral and vertical facies differentiation of sand and limestone of Badenian age, which is described in more detail in the geology section. For the ERT survey the Wenner-α-array was applied. Due to geometry factors, this array is very sensitive to horizontal changes in resistivity (Barker 1979), which was expected based on the outcrop observations (Fig. 7).

In conclusion, a two-layer structure comprising a lower resistivity layer at the base and a higher resistivity layer with resistivity change in both horizontal and vertical directions can be derived. An up to 10 m thick lower layer is characterized by resistivities lower than 200 ohm m, which in comparison with the outcrop (Fig. 7b) is interpreted as sand of Badenian age, the main facies of the Oslip sand pit. In the upper part of the profile a higher resistivity layer (400–600 ohm m) of a few meters in thickness increases to about 6–7 m to the southeast, where from profile meter 70–90 the highest resistivities exceeding 1,000 ohm m occur. To sum up, this top layer changes laterally in a southeastern direction from coarse-clastic beds in the northern part (Fig. 7c) to a massive limestone breccia (Fig. 7d), which turns to Leitha Limestone farther to the southeast.

ERT profile along the road Oslip–Rust

The subsurface of the first 400 profile meters (Fig. 12)—with resistivities ranging from 200 to 1,500 ohm m are interpreted as fluvial deposits of a paleo riverine of Quaternary age. It is underlain by low resistivity beds (<30 ohm m) down to the maximum penetration depth of approximately 30–35 m, which are interpreted as fine-clastic beds of Pannonian age. The coarse-clastic deposits reach down to a depth of 5–10 m, and increase in thickness towards profile meter 350. The higher resistivities of 400–1,500 ohm m are interpreted as gravel deposited by a paleo Wulka River. At profile meter 350 a sharp, steep offset of about 8 m occurs, separating the Quaternary gravel beds from very low

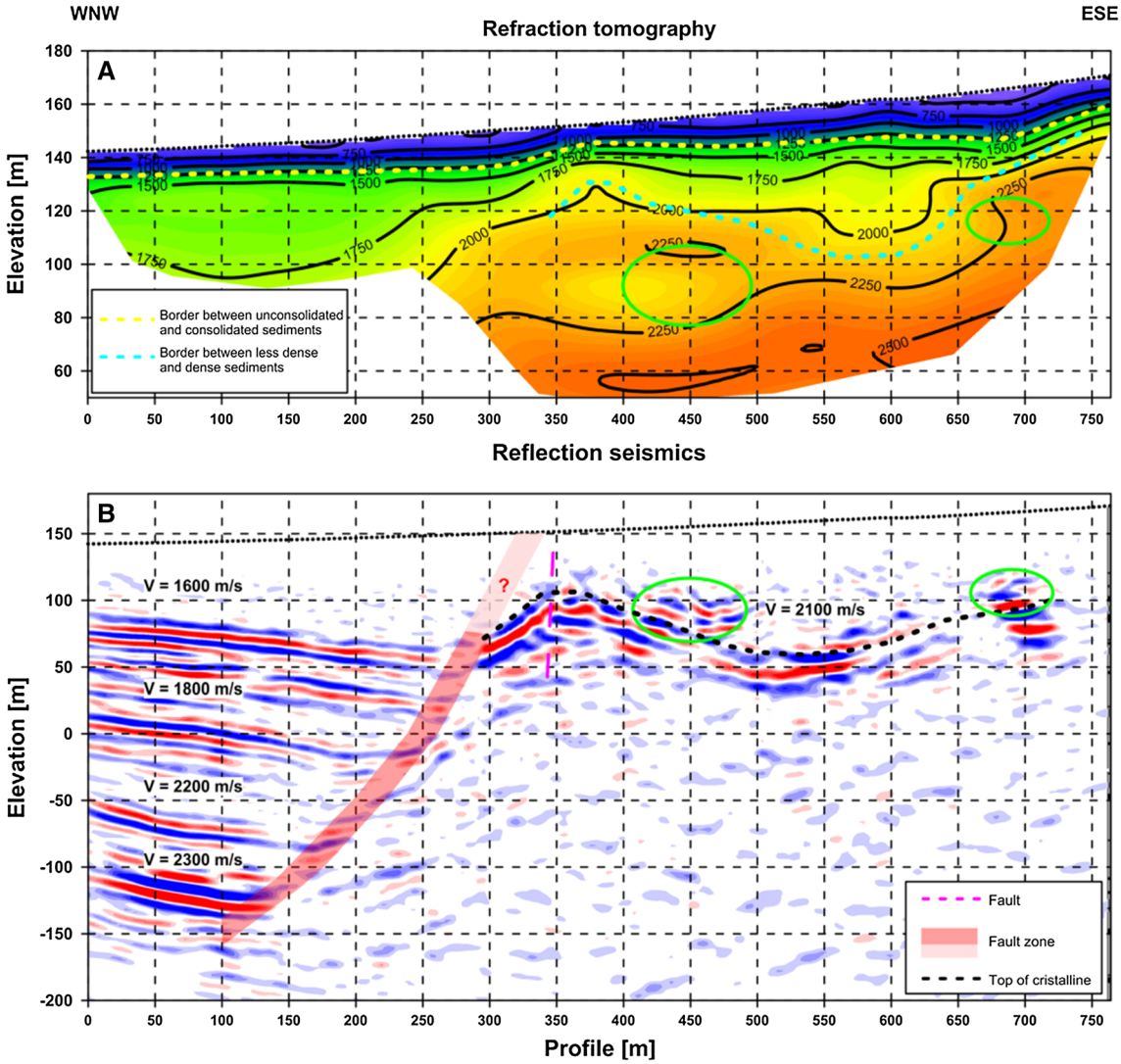

Fig. 13 Results of the refraction tomography (scale 1:2) and reflection seismics (scale 1:1) of the road section Oslip–Rust, along with structural interpretation. *Yellow dotted line* marks border between less consolidated and consolidated deposits. *Light blue dotted line* marks significant change in density. *Yellow ellipses* mark higher velocities in the refraction profile (**a**) corresponding to multiple reflections in the reflection profile (**b**). The thickness of the damage zone of the listric fault is marked by a *question mark*

resistivities. This approximately 100 m long low resistivity zone is interpreted as a prominent fault zone, separating the marl and clay of Pannonian age from the (water saturated) sandy gravel of the Rust Formation, which underlies the faulted Leitha Limestone of Badenian age.

This sharp boundary coincides with both the prominent fault in the geological map (Fig. 3) and the deep fault structure of the seismic section (Fig. 13). Due to missing outcrops, no decision was possible as to whether the gradually eastward thickening of the high resistivity deposits of Quaternary age was caused by cut bank erosion of a paleo riverine and subsequent fill with coarse clastic deposits, or by a continuation of Neogene subsidence in Quaternary times. However, very young fault structures in the St. Margarethen quarry (Kieslinger 1955, 1960) and historical earthquakes such as in the year 1766 with an EMS-98 intensity of 7 (Häusler 2010) indicate pronounced fault tectonic activity in the vicinity of the St. Margarethen Fault zone.

From profile meter 350–500 the ERT profile shows resistivity values ranging from 70 to 150 ohm m. These could be interpreted as Pannonian deposits but correspond to mapped deposits of the Rust Formation.

An undulated and sliced high resistivity body (200–2,000 ohm m) with a clear boundary to lower resistivity beds at its base can be found from profile meter 570–850, which matches the Leitha Limestone of Badenian age. Based on detailed geologic mapping (Fig. 3) and the local

geophysical investigations at the Oslip sand pit (Fig. 11) the lower resistivity zones within this high resistivity body are interpreted as change from limestone facies to detritic facies of Badenian age. It is unclear, however, if internal abrupt changes of resistivity at profile meter 670–700 and 850–870 are due to local tectonic faults or to rapid facies change from limestone- to sand-facies. As Zhu et al. (2009) pointed out, buried faults can be recognized by low resistivity zones extending into depth, in particular for water-saturated zones, which is the situation in the Rust Formation.

The eastern termination of the high resistivity body at profile meter 850 is interpreted as a tectonic fault separating the Leitha Limestone of Badenian age from the fluvial Rust Formation of Karpatian age to the east. Due to apparently similar low resistivities of the clastic formation of Badenian age and the probably groundwater-saturated sandy gravel of the Rust Formation, it is not possible to draw a clear boundary separating the Badenian formations from the underlying Rust Formation. Due to weak differences in the resistivity of the Neogene formations, the St. Margarethen Fault cannot clearly be identified in the shallow ERT profile, which can however clearly be traced in the seismic section.

Seismics

The resistivity distribution of Neogene deposits in the ERT profile down to a depth of 30 m is directly followed up by the velocity information of the seismic profile down to a depth of 350 m. Table 4 gives an overview on velocities of hard- and soft-rocks known from previous seismic investigations in the region (e.g. Kohlbeck 1995; Häusler 2010).

Down to a depth of 15 m the refraction tomography (Fig. 13a) reveals a low velocity layer with velocities below 1,200 m/s probably corresponding to weathered hard rock or unconsolidated soft rock. In a depth of about 5–15 m, a high vertical velocity gradient marks an abrupt velocity change, which indicates consolidated deposits (yellow dotted line), whose greater thickness corresponds to high resistivity patterns in the ERT profile. Profile meter 300 reveals a significant change in lateral velocity. To the west, lower velocities in the range of 1,600–2,000 m/s were measured down to an altitude of 90 m, which are interpreted as marl and clay deposits of the eastern Eisenstadt Basin. Higher velocities between profile meter 350 and 400 reach close to the surface and towards profile meter 600 dip down again to an altitude of 150 m forming a depression, which is marked by a light blue dotted line. Two zones of high velocity (2,250 m/s) between profile meters 400–500 at an altitude of 90 m and at profile meter 680 at an altitude of 110 m are marked by yellow ellipses, which correspond to multiple reflections of the reflection profile indicating that dense sediments underlie more loose deposits. The contact between sedimentary deposits and the crystalline basement of the Rust Range is not well defined along the whole profile but the velocities ranging from 2,250 to 2,500 m/s show that the crystalline must be strongly faulted or weathered.

Table 4 General velocities of hard- and soft-rock formations in the eastern Eisenstadt Basin

Velocity (m/s)	Formation (age)
1,600	Marl and clay (Pannonian)
1,800–2,300	Gravel, sand, marl (Badenian–Sarmatian)
2,100 and more	Leitha Limestone (Badenian–Sarmatian)
2,200 and more	Rust Formation (Karpatian)
>2,500	Crystalline basement

Along the first 300 profile meters the reflection seismic (Fig. 13b) down to a depth of approximately 300 m (equaling an altitude of −150 m) shows a sequence of reflectors slightly dipping towards the east. The interval velocities of the layers between the major reflectors increase with depth from 1,600 to 2,300 m/s, and these layers definitely increase in thickness towards the east up to approximately 15 m. The deepest reflector of this profile is (still) a sediment layer in a depth of approximately 300 m is still a sediment layer. This can be derived from gravimetry (Fig. 14), but also from an unpublished seismic profile taken several kilometers to the west (Scheibz 2010), which is made up of thick sedimentary beds down to a depth of 750 m. Towards the crystalline of the Rust Range the inclined reflectors either bow up or terminate. Consequently, two curved faults paralleling each other belonging to the St. Margarethen Fault zone can be interpreted. The geometry of the reflectors indicates the existence of a listric high angle normal fault. East of this fault zone at profile meter 300 the crystalline is either weathered or strongly faulted. At profile meter 350 a nearly vertical fault is depicted in the crystalline basement, which corresponds to low resistivities in the ERT-profile.

Between profile meters 400–500, approximately 60 m below surface (at 100 m above sea level) and between 680 and 710 approximately 45 m below surface (at 125 m above sea level) a package of reflections is characterized by a higher velocity of about 2,100 m/s. These areas are marked by yellow ellipses, and can be interpreted as denser deposits of the Rust Formation covering the crystalline basement. The refraction tomography along this undulated reflector, highlighted as a dotted light blue line, indicates that the basal Neogene deposits of the Rust Range reveal a concave structure. However, fold structures cannot be clearly traced in the reflection profile.

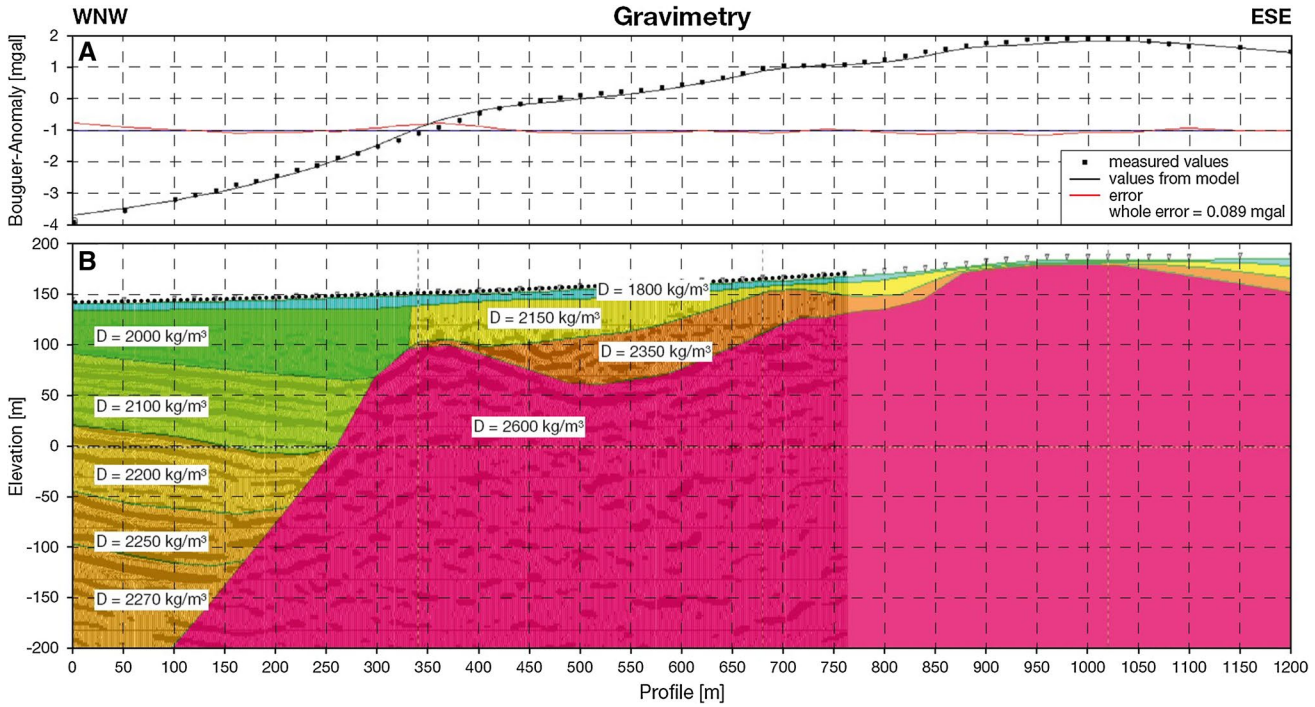

Fig. 14 Bouguer-anomaly, model anomaly, model error (**a**), and density model along the Oslip road section (**b**). *D* density of soft- and hard-rock formations

Table 5 Density distribution of soft- and hard-rock formations in the eastern Eisenstadt Basin

Density (kg/m^3)	Formation (age)
2,000–2,100	Marl and clay (Pannonian)
2,200–2,270	Gravel, sand, marl (Badenian to Sarmatian)
2,150	Leitha Limestone (Badenian to Sarmatian)
2,350	Rust Formation (Karpatian)
2,600	Crystalline basement

Gravimetry

In order to get a reasonable local density model the reflection seismic image and the refraction tomography was underlain by the density model, and the interval seismic velocity was used to estimate the densities of the layers (Table 5). Thereafter the geometries and densities of the layers were adapted until the gravimetric effect of the model fit to the Bouguer-anomaly. The final error is 0.089 mgal.

At the beginning of the profile the density model shows eastward inclined deposits with densities increasing with depth from 2,000 to 2,270 kg/m^3 (Fig. 14b). The border to the hard rock of the crystalline basement is well defined through gravimetry; it is steep nearer to the surface and flattens in greater depths. Moreover, it is obvious that the last visible reflector of the seismic overlay at an elevation of −100 m is not the crystalline but a deep sediment layer. Consequently, at the beginning of the profile, the crystalline basement deepens to more than 400 m, which is not presented in this profile. Between profile meter 350 and 750 a depression is filled with sediments of higher densities, which corresponds to the denser deposits of the Rust Formation. Between profile meter 900 and 1,050 the crystalline basement reaches the subsurface, but declines again towards profile meter 1,200 in the east.

Discussion and conclusions

At this point the St. Margarethen Fault and formation of the Eisenstadt Basin as well as structures of the Rust Range shall be put in context to essential steps of the formation of the Vienna Basin and its Austroalpine frame. Eastward lateral extrusion of a major Alpine-Carpathian block in Miocene times (Salcher et al. 2012) resulted in the opening of the pull-apart Vienna Basin to a width of at least 10 km along bended left lateral strike-slip faults. In the Late Karpatian, thrusting developed into lateral extrusion, and this change in tectonic regime is locally documented as a major regressive event during which fluvial systems entered the Vienna Basin from the south. Younger sedimentary gaps and unconformities during Lower and Upper Miocene

times are well documented throughout the Vienna Basin and Eisenstadt Basin. They represent erosional structures related to sea-level drops at the base of the Rust Formation as well as during Upper Badenian to Sarmatian times like Strauss et al. (2006) have pointed out for the Vienna Basin.

Based on mapping Lower Miocene formations on top and around the Leitha Mountains the exploration geologist Kölbl (1952) described this northeast-trending Austroalpine range as updoming ("geotektonische Aufwölbungszone"). Tollmann (1985) followed this interpretation and concluded a 200-m Miocene updoming of the Leitha Mountains. The Hainburg Mountains form the northeastern continuation of the Austroalpine basement of the Leitha Mountains and are also characterized by prominent Lower Miocene unconformities. Wessely (1961) described wide fractures in Leitha Limestone of Badenian age sealed by Upper Sarmatian clastics. Hence, he concluded a post-Badenian updoming of the Hainburg Mountains of approximately 210 m, which matches the range of updoming of the Leitha Mountains. The total post-Badenian updoming of the Austroalpine frame southeast of the Vienna Basin is therefore about 200 m.

Since the area of the Hainburg Mountains, east of the maximum opening of the pull-apart Vienna Basin, in Late to Post-Sarmatian times was affected by an uplift of another 100 m (Wessely 1961), there seems to be a relation between lateral width of Vienna Basin pull-apart opening and the amount of concurrent uplift of the adjacent Austroalpine frame. In conclusion, the Miocene extension of the Vienna Basin and the subsidence of the Eisenstadt Basin coevally were accompanied by concurrent updoming of their Austroalpine frame comprising the Leitha- and Hainburg-Mountains, Rust Range and Lake Neusiedl region at a time when the Neusiedl Basin did not yet exist as a sub-basin of the Danube Basin.

Based on these considerations the structures of the geophysical section are discussed (Fig. 15) and results are drawn in a geological profile (Fig. 16). The master fault depicted in the seismic section separates the Rust Range from the Neogene of the Eisenstadt Basin (Fig. 15). The western section of the seismic profile clearly reveals reflectors, which are interpreted as eastward dipping and eastward thickening beds of Upper Miocene age, and in combination with the density model the fault zone is characterized by a decreasing angle of dip with depth representing a curved surface with its concave upward and thus can be termed a listric fault (Shelton 1984). The low resistivity zone between ERT-profile meters 350–400 is followed by a broader zone down to a depth of 350 m, which can be interpreted as a fault damage zone, along which the deposits of the eastern Eisenstadt Basin slid down the western margin of the Rust Range. The reflectors of the seismic section east of the St. Margarethen Fault, between profile meter 450 and 750 and at a depth of approximately 100 m above sea level, are undulated and parallel each other. This undulated structure east of the St. Margarethen Fault probably represents a folded crystalline basement overlain by clastics of the Rust Formation. The eastern continuation of this undulated structure at the Neogene base can be derived from the gravimetric profile, which clearly reveals a concave structure with its crest on top of the Rust Range (Fig. 13a). Since folding of Neogene formations along the Rust Range can be excluded, the undulated base of Rust Formation probably marks a pre-Karpatian relief filled up by fluvial deposits.

Since Neogene succession on top of the northern Rust Range reaches up to Leitha Limestone of Middle Badenian age and since the margins of the Range are unconformably overlain by Leitha Limestone of Upper Sarmatian age, epirogenetic uplift of the Rust Range during Upper Badenian to Sarmatian times is concluded. Comparison of the present altitude of the base of Badenian Leitha Limestone on top of the Rust Range (200 m above sea level) with its base at the eastern and western margin (130 m above sea level) leads to the conclusion of an uplift of the central Rust Range of at least 70 m. In the St. Margarethen quarry, about 2, 5 km to the south, Leitha Limestone forms an antiform with an axis in north–south direction plunging gently to the south and conjugate pairs of faults, which compensated for the tension caused by updoming (Sauer et al. 1992b; Figs. 79–81). The exploration well Zillingtal 1 in the western Eisenstadt Basin, reaching to a depth of 1,415 m, proves 1,150 m thick deposits of Badenian age overlain by approximately 200 m thick deposits of Sarmatian age. In conclusion, continuous subsidence of the Eisenstadt Basin coevalled the period of updoming of the Rust Range during Lower Miocene times. Ongoing subsidence of the Eisenstadt Basin along the listric master fault in front of the uplifted Rust block during Upper Miocene times resulted in growth-strata dipping to the east and fault drags indicate a hanging-wall syncline.

Uplift during hanging wall subsidence is suggested as the mechanism of the updoming of the Rust Range footwall. Subsidence of eastern Eisenstadt Basin in front of Rust Range to a depth 400 m in total probably took place along one single north–south-trending master fault. This fault was then dissected, when the Rust block was separated from the Oslip block (Fig. 3). As a consequence, Upper Sarmatian growth-strata at the western margin of the Rust block were uplifted and therefore exposed in the gravel pit of the St. Margarethen–Gemeindewald. The synoptic interpretation of the geophysical profile along the Oslip section reveals that a listric fault must not necessarily decline into a weak layer serving as ductile detachment horizon, since the depth of the eastern Eisenstadt Basin of approximately 400 m was to shallow for flattening into any of Neogene layers (Fig. 2).

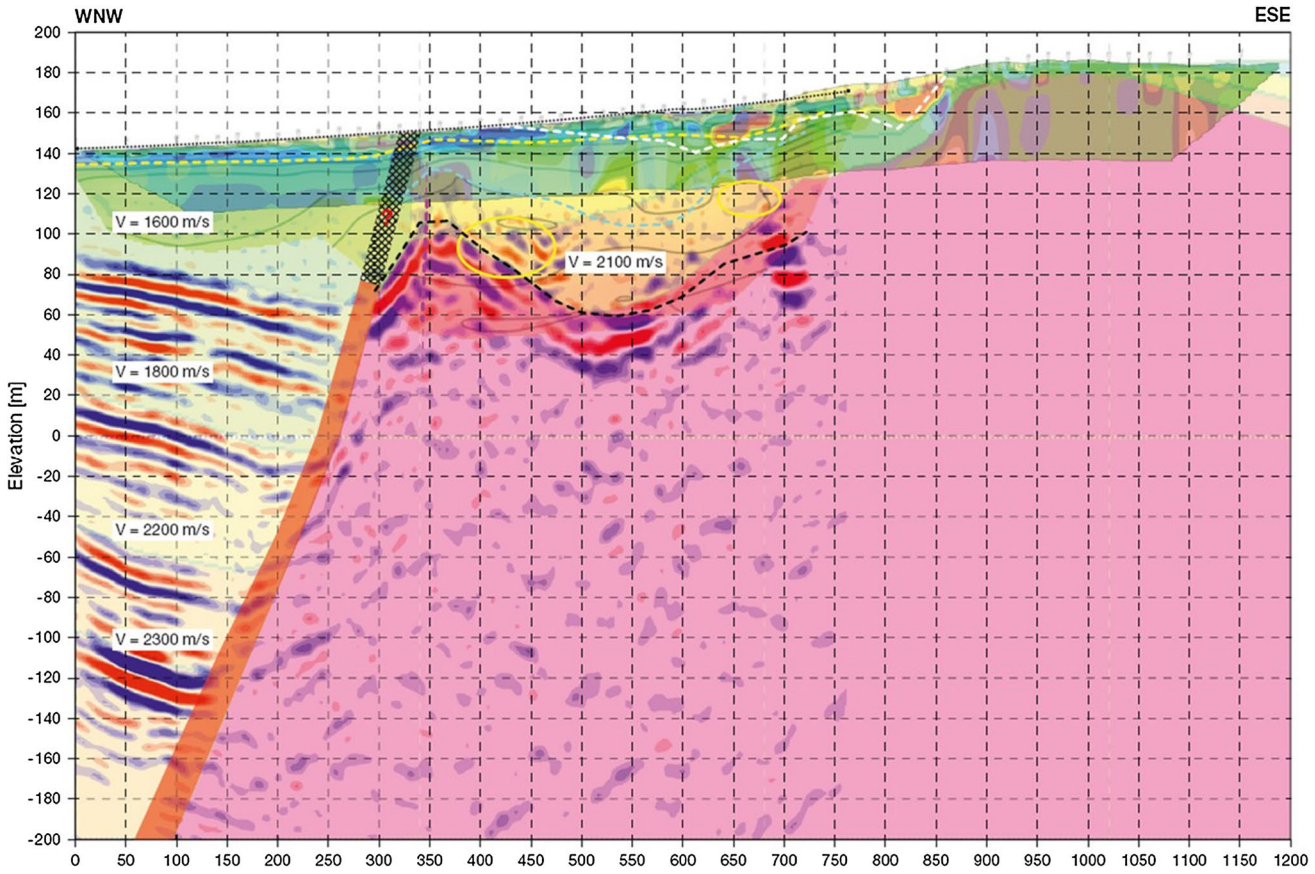

Fig. 15 Synoptic view of gravimetric-, seismic- and ERT-profile along the road Oslip–Rust (Figs. 12, 13, 14) at same *scale*. The St. Margarethen Fault zone is drawn as fault damage zone, which separates the Miocene growth-strata and syncline of the Eisenstadt Basin in the west from the Rust Range in the east

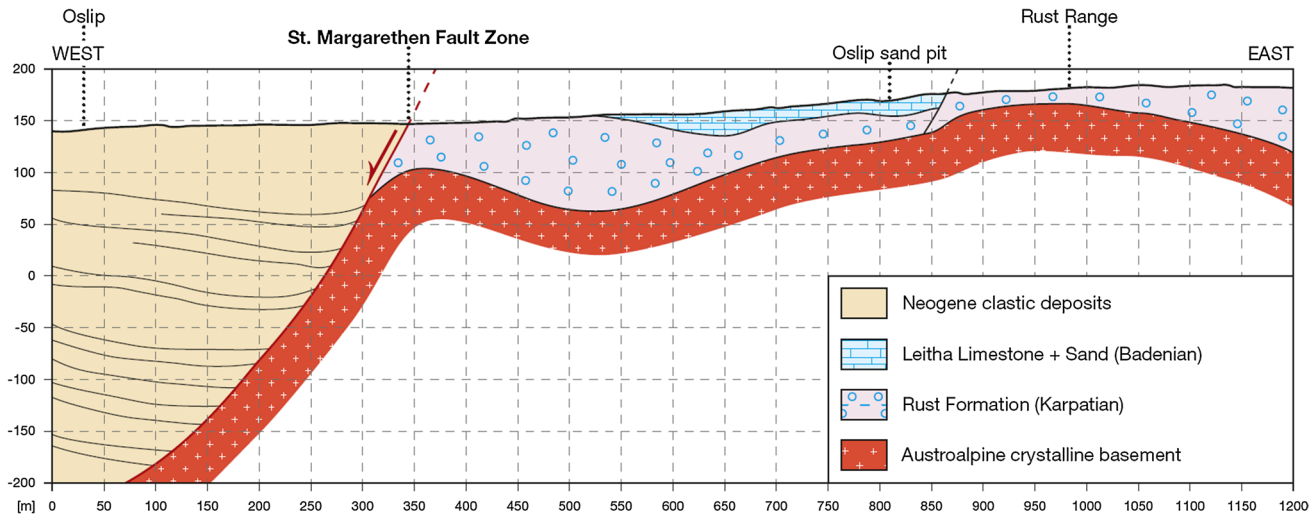

Fig. 16 Geological profile drawn based on the geophysical sections overlain in Fig. 15

Acknowledgments The authors thank Godfrid Wessely and one anonymous reviewer for constructive and thorough reviews.

References

Ahl A, Bieber G, Motschka K, Römer A, Slapanski P, Supper R (2012) Aerogeophysikalische Vermessung im Bereich Leithagebirge (Bgld.). Ber Geol Bundesanst, Wien

Barker RD (1979) Signal contribution sections and their use in resistivity studies. Geophys J R Astron Soc 59:123–129

Brix F, Pascher GA (1994) Geologische Karte der Republik Österreich 1:50.000, Blatt 77 Eisenstadt. Geologische Bundesanstalt, Wien

Decker K (1996) Miocene tectonics at the Alpine–Carpathian junction and the evolution of the Vienna Basin. Mitt Ges Geol Bergbaustud Österr 41:33–44

Decker K, Peresson H (1996) Rollover and hanging-wall collapse during Sarmatian/Pannonian synsedimentary extension in the Eisenstadt Basin. Mitt Ges Geol Bergbaustud Österr 41:45–52

Decker K, Peresson H, Hinsch R (2005) Active tectonics and Quaternary basin formation along the Vienna Basin transform fault. Quat Sci Rev 24:307–322

DeGroot-Hedlin C, Constable S (1990) Occam's inversion to generate smooth, two dimensional models from magnetotelluric data. Geophysics 55:1613–1624

Exner U, Grasemann B (2010) Deformation bands in gravels: displacement gradients and heterogenous strain. J Lond Geol Soc 167:905–1013

Exner U, Rath A (2012) Deformationsbänder im Leithakalk. Wiss Arb Burgenland 142:51–54

Exner U, Rath A, Grasemann B, Draganits E (2008) Soft-sediment deformation and deformation of porous sand: structural highlights in the southern Vienna and Eisenstadt Basin. J Alp Geol 49:129–136

Feichtinger F, Spörker H (1996) ÖMV–OMV: Die Geschichte eines österreichischen Unternehmens. Ferdinand Berger & Söhne, Horn

Fuchs W (1960) Geologischer Bau und Geschichte des Ruster Berglandes. Dissertation, Universität Wien

Fuchs W (1965) Geologie des Ruster Berglandes (Burgenland). Jb Geol Bundesanst 108:155–194

Grasemann B, Martel S, Wiesmayr G (2004) Unconstrained listric faults. Ber Inst Erdwiss Karl-Franzens-Univ Graz 9:151–153

Grasemann B, Martel S, Passchier C (2005) Reverse and normal drag along a fault. J Struct Geol 27:999–1010

Harzhauser M, Piller WE (2005) Neogen des Wiener Beckens. 75. Jahrestagung der Paläontologischen Gesellschaft, Graz

Harzhauser M, Tempfer PM (2004) Late Pannonian wetland ecology of the Vienna Basin based on mollusces and lower vertebrate assemblages (Late Miocene, MN 9, Austria). Cour Forsch Senckenberg 246:55–68

Harzhauser M, Kowalke T, Mandic O (2002) Late Miocene (Pannonian) gastropods of Lake Pannon with special emphasis on early ontogenetic development. Ann Naturhist Mus Wien 103A:75–141

Harzhauser M, Daxner-Höck G, Piller WE (2004) An integrated stratigraphy of the Pannonian (Late Miocene) in the Vienna Basin. Aust J Earth Sci 95(96):6–19

Häusler H (2007) Geologische Karte der Republik Österreich 1:50.000, Erläuterungen zu den Blättern 79 Neusiedl am See, 80 Ungarisch-Altenburg und 109 Pamhagen. Geologische Bundesanstalt, Wien

Häusler H (2010) Geologische Karte der Republik Österreich 1:50.000, Erläuterungen zur Geologischen Karte 78 Rust. Geologische Bundesanstalt, Wien

Häusler H (2012a) Contribution to the discussion of folded Pannonian strata in the Southern Vienna Basin. Geophys Res Abstr 14:EGU2012-5201

Häusler H (2012b) Folded Pannonian beds along the Austroalpine frame of the southern Vienna Basin. Pangeo Austria Abstr 55–56

Häusler H, Leber D, Peresson H, Hamilton W (2002) A new exploration approach in a mature basin—integration of 3-D seismic, remote sensing, and microtectonics, southern Vienna Basin, Austria. In: Schuhmacher H, LeSchak LA (eds) Surface exploration case histories. Application of geochemistry, magnetics and remote sensing. American Association of Petroleum Geologists Studies in Geology 48, SEG Geophysical References Series 11, Tulsa, Oklahoma, pp 433–451

Häusler H, Scheibz J, Kohlbeck F, Kostial D, Chwatal W (2007) Complementary geophysical investigations revealing camouflaged tectonic structures in the Northern Burgenland (Austria). Geopys Res Abstr 9:EGU2007-03754

Häusler H, Mörtl G, Wagner S, Körner W, Rank D, Papesch W, Payer T, Scheibz J, Tschach M (2008a) The complex aquifer system of Schützen am Gebirge (Northern Burgenland, Austria). J Alp Geol 49:39

Häusler H, Scheibz J, Payer T, Körner W, Rank D, Papesch W, Faber R, Weixelberger G (2008b) Is fault geometry or Miocene facies controlling the aquifer geometry? Results from the Lackenbach case study (Northern Burgenland, Austria). J Alp Geol 49:38–39

Herrmann P, Pascher GA, Pistotnik J (1993) Geologische Karte der Republik Österreich 1:50.000, 78 Rust. Geologische Bundesanstalt, Wien

Hölzel M, Wagreich M, Faber R, Strauss P (2008) Regional subsidence analysis in the Vienna Basin (Austria). Aust J Earth Sci 101:89–98

Hölzel M, Decker K, Zámolyi A, Strauss P, Wagreich M (2010) Lower Miocene structural evolution of the central Vienna Basin (Austria). Mar Petrol Geol 27:666–681

Kardeis G (2009) Evaluierung geoelektrischer Tiefensondierungen im Neogen und Pleistozän des nördlichen Burgenlandes. Universität Wien, Diplomarbeit

Kieslinger A (1955) Rezente Bewegungen am Ostrande des Wiener Beckens. Geol Rdsch 43:178–181

Kieslinger A (1960) Die Spaltenhöhlen von St. Margarethen im Burgenland. Wiss Arb Burgenland 25:7–9

Kohlbeck F (1995) Bericht über geophysikalische Untersuchungen zur Erkundung mineralhältiger Wässer im Gemeindegebiet von Mörbisch. Technische Universität, Wien

Kölbl L (1952) Bericht über die geologische Kartierung im Jahre 1952, Gebiet: Nordwestrand des Leithagebirges zwischen Hof und Kaisersteinbruch; Südostabfall des Leithagebirges von Breitenbrunn bis Neusiedl und Teile der Parndorfer Platte. Arch Geologische Bundesanstalt, Wien

Kollmann W (2005) Wasserwirtschaftliche Untersuchungen im Grenzraum zu Ungarn, Bereich St. Margarethen–Siegendorf–Mörbisch/Sopron. Geologische Bundesanstalt, Wien

Kröll A, Wessely G (1993) Strukturkarte - Basis der tertiären Beckenfüllung 1:200.000. Erläuterung zu den Karten über den Untergrund des Wiener Beckens und der angrenzenden Gebiete. Geologische Bundesanstalt, Wien

Küpper H (ed) (1957) Erläuterungen zur geologischen Karte Mattersburg – Deutschkreuz 1:50.000. Geologische Bundesanstalt, Wien

Loke MH (2004) Tutorial: 2-D and 3-D electrical imaging surveys (pdf). http://www.ualberta.ca. Retrieved 27 Oct 2014

Peresson H, Decker K (1996) From extension to compression: Late Miocene stress inversion in the Alpine–Carpathian–Pannonian transition area. Mitt Ges Geol Bergbaustud Österr 41:75–86

Peresson H, Decker K (1997) Far field effects of Late Miocene subduction in the Eastern Carpathians: E–W compression and inversion of structures in the Alpine–Carpathian–Pannonian region. Tectonics 16:38–56

Piller WE, Harzhauser M (2005) The myth of the Brakish Sarmatian sea. Terra Nova 17:450–455

Pretsch H (2009) Deformation an sarmatischen Sedimenten (St. Margarethen/Burgenland). Diplomarbeit, Universität Wien

Rath A, Exner U, Tschegg C, Grasemann B, Laner R, Draganits E (2011) Diagenetic control of deformation mechanisms in deformation bands in a carbonate grainstone. Am Assoc Pet Geol B95:1369–1381

Sacchi M, Horváth F (2002) Towards a new time scale for the Upper Miocene continental series of the Pannonian basin (Central Paratethys). EGU Stephan Mueller Spec Publ Ser 3:79–94

Salcher BC (2008) Sedimentology and modelling of the Mitterndorf Basin. Dissertation, Universität Wien

Salcher BC, Meurers B, Smit J, Decker K, Hölzel M, Wagreich M (2012) Strike–slip tectonics and Quaternary basin formation along the Vienna Basin fault system inferred from Bouguer gravity derivates. Tectonics 31:TC3004

Sauer R, Seifert P, Wessely G (1992a) Part I: outline of sedimentation, tectonic framework and hydrocarbon occurrence in eastern Lower Austria. Mitt Österr Geol Ges 85:5–96

Sauer R, Seifert P, Wessely G (1992b) Part II: excursions. Mitt Österr Geol Ges 85:97–239

Sauerzopf F (1962) Die Brunnenwässer der Freistadt Rust am See. Wiss Arb Burgenland 29:124–131

Scheibz J (2006) Geologisch-geophysikalische Untergrunduntersuchungen im Gebiet Schützen am Gebirge (Nordburgenland). Diplomarbeit, Universität Wien

Scheibz J (2010) Geologisch-geophysikalische Untersuchung postmiozäner Strukturen zwischen Leithagebirge und Ruster Höhenzug (Nördliches Burgenland). Dissertation, Universität Wien

Scheibz J, Häusler H, Kardeis G, Heischmann J, Kopecny A (2008a) The Schützen "hot spot": 3D-modelling of a shallow aquifer (Northern Burgenland, Austria). J Alp Geol 49:93

Scheibz J, Häusler H, Kohlbeck F, Chwatal W, Kostial D (2008b) Geologic interpretation of shallow and deep geophysical soundings in the section Leithagebirge – Ruster Höhenzug (Northern Burgenland, Austria). J Alp Geol 49:93–94

Scheibz J, Häusler H, Kardeis G, Kohlbeck F, Chwatal W, Figdor H, König C (2009) Geologic interpretation of geophysical investigations in the Oslip section, Rust Range, Northern Burgenland, Austria. Geophys Res Abstr 11:EGU2009-10559

Schmid H (1968) Zur Hydrogeologie der Kaliquellen des Neusiedlerseegebietes unter besonderer Berücksichtigung der Verhältnisse um Rust. Wiss Arb Burgenland 40:17–21

Schuster R (2010) Unterostalpin. In: Häusler H (ed) Geologische Karte der Republik Österreich 1:50.000, Erläuterungen zur Geologischen Karte 78 Rust. Geologische Bundesanstalt, Wien

Schuster GT, Quintus-Bosz A (1993) Wavepath eikonal traveltime inversion: theory. Geophysics 58:1314–1323

Shelton JW (1984) Listric normal faults: an illustrated summary. Am Assoc Pet Geol B68:801–815

Smith RC, Sjogren DB (2006) An evaluation of electric resistivity imaging (ERI) in Quaternary sediments, southern Alberta, Canada. Geosphere 2:287–298

Spahić D, Exner U, Behm M, Grasemann B, Haring A, Pretsch H (2011) Listric versus planar normal fault geometry: an example from the Eisenstadt-Sopron Basin (E Austria). Int J Earth Sci 100:1685–1695

Spiegel RJ, Sturdivant VR et al (1980) Modeling resistivity anomalies from localized voids under irregular terrain. Geophysics 45:1164–1183

Strauss P, Harzhauser M, Hinsch R, Wagreich M (2006) Sequence stratigraphy in a classic pull-apart basin (Neogene, Vienna Basin). A 3D based integrated approach. Geol Carpathica 57:185–197

Székely B, Zámolyi A, Draganits E, Briese C (2009) Geomorphic expression of neotectonic activity in a low relief area in an Airborne Laser Scanning DTM: a case study of the Little Hungarian Plain (Pannonian Basin). Tectonophysics 474:353–366

Tollmann A (1977) Geologie von Österreich, 1, Zentralalpen. Deuticke, Wien

Tollmann A (1985) Geologie von Österreich, 2, Außerzentralalpiner Anteil. Deuticke, Wien

Wessely G (1961) Geologie der Hainburger Berge. Jahrb Geol Bundesanstalt 104:273–349

Wessely G (2006) Niederösterreich. Geologische Bundesanstalt, Wien

Wiedl G, Harzhauser M, Piller WE (2012) Facies and synsedimentary tectonics on a Badenian carbonate platform in the southern Vienna Basin (Austria, Central Paratethys). Facies 58:523–548

Zhu T et al (2009) The application of electrical resistivity tomography to detecting a buried fault: a case study. J Environ Eng Geophys 14:145–151